Cross-correlation spectroscopy study of the transient spark discharge in atmospheric pressure air

2017 Plasma Sources Sci. Technol. 26 055010

(http://iopscience.iop.org/0963-0252/26/5/055010)

IOP Publishing

Plasma Sources Science and Technology

Plasma Sources Sci. Technol. **26** (2017) 055010 (8pp)

https://doi.org/10.1088/1361-6595/aa642a

Cross-correlation spectroscopy study of the transient spark discharge in atmospheric pressure air

Mário Janda[1], Tomáš Hoder[2], Abdollah Sarani[3], Ronny Brandenburg[3] and Zdenko Machala[1]

[1] Faculty of Mathematics, Physics and Informatics, Comenius University in Bratislava, Mlynská dolina F2, 842 48 Bratislava, Slovakia
[2] Faculty of Science, Masaryk University, Kotlarska 2, 611 37 Brno, Czechia
[3] INP Greifswald e.V., Felix-Hausdorff-Str. 2, D-17489 Greifswald, Germany

E-mail: janda@fmph.uniba.sk

Received 9 November 2016, revised 2 February 2017
Accepted for publication 2 March 2017
Published 31 March 2017

CrossMark

Abstract

A streamer-to-spark transition in a self-pulsing transient spark (TS) discharge of positive polarity in air was investigated using cross-correlation spectroscopy. The entire temporal evolution of the TS was recorded for several spectral bands and lines: the second positive system of N_2 (337.1 nm), the first negative system of N_2^+ (391.4 nm), and atomic oxygen (777.1 nm). The results enable the visualization of the different phases of discharge development including the primary streamer, the secondary streamer, and the transition to the spark. The spatio-temporal distribution of the reduced electric field strength during the primary streamer phase of the TS was determined and discussed. The transition from the streamer to the spark proceeds very fast within about 10 ns for the TS with a current pulse repetition rate in the range 8–10 kHz. This is attributed to memory effects, leading to a low net electron attachment rate and faster propagation of the secondary streamer. Gas heating, accumulation of species such as oxygen atoms from the previous TS pulses, as well as generation of charged particles by stepwise ionization seem to play important roles contributing to this fast streamer-to-spark transition.

Keywords: cross-correlation spectroscopy, transient spark, streamer-to-spark breakdown mechanism, atmospheric air discharge

(Some figures may appear in colour only in the online journal)

1. Introduction

The transition from the streamer to the secondary streamer and finally to the heated channel leading to spark breakdown in air are phenomena of general importance, for example when working with various atmospheric pressure electrical discharges, as well as in the design of high voltage (HV) devices. The first studies of the atmospheric pressure air breakdown mechanism appeared several decades ago [1–3] and the streamer breakdown theory was introduced by Meek [4], Raether [5] and Loeb [6] in the middle of the 20th century. However, because of the complexity of this problem, investigations of the breakdown mechanism, streamers and their propagation have continued up to nowadays [7–12].

We investigated a relatively novel type of atmospheric pressure discharge, named the transient spark (TS) [13–15]. The TS is a dc-operated, self-pulsing and filamentary discharge with typical repetition rate in the range 1–10 kHz. Fundamental research of the TS characteristics revealed that it is initiated by a primary streamer, followed by a secondary streamer generating the short current pulse [13–17]. Current pulses have maximum amplitude in the range of a few Amps, but are sufficiently short (~10–100 ns). Thus, significant heating of the treated gas is avoided and the generated plasma is non-equilibrium and highly reactive, with an electron density up to approximately 10^{17} cm^{-3} [18].

The gas breakdown leading to the spark formation is not desired in many electrical discharges and non-thermal plasma applications but, periodic streamer-to-spark transition with restricted spark phase like in the TS can bring multiple benefits in various applications of non-thermal plasmas, such as local and transient elevation of the gas temperature, formation of hydrodynamic expansion and production of reactive species in high concentrations [9, 17, 19–21]. However, the control of power dissipation and discharge inception is still not fully understood and the TS represents an excellent object for the study of the rapid streamer-to-spark transition. This is not only an issue for new plasma applications, but also for explanation of phenomena like lightning or transient luminous event in the upper atmosphere [22–25]. Despite different time and length scales, similar discharge evolution and characteristics can be expected there.

In particular, further fundamental research of TS is needed, e.g. for the explanation of TS peculiarities as they change with increasing pulse repetition frequency [14, 16]. Based on the significant shortening of the streamer-to-spark transition delay time [16], a change of the breakdown mechanism in the TS with the increasing pulse repetition frequency is assumed. There are probably several 'memory' effects (especially preheating, residual ions, and changes of the gas composition by previous TS pulses) in the gap. Residual space charges may also influence the discharge development, similar as obtained in dielectric barrier discharge with electrode's geometry generating subsequent single discharge filaments at the same location [26].

The time-resolved imaging using intensified CCD cameras provides information about the various streamer characteristics, such as propagation velocity, branching, or channel thickness [27–29]. Even the propagation of a single discharge event can be detected using several synchronized intensified CCD cameras [26]. Fast streak cameras and cross-correlation spectroscopy (CCS) enable a more detailed and time-resolved information about the evolution of transient discharge events [30, 31]. In this paper we explore the entire evolution of the TS discharge from the primary streamer to the spark breakdown at a pulse repetition frequency in the range 8–10 kHz. CCS was used [32, 33], since it is very sensitive and suitable for the investigation of self-pulsing and strongly erratic appearing discharges. Other techniques like intensified CCD cameras require precise external synchronization with the discharge event and do not achieve sufficiently high temporal resolution and sensitivity.

2. Experimental setup

The positive polarity TS was generated in dry atmospheric pressure air between steel electrodes in point-to-plane configuration. The gap length was 4 mm. The DC HV power supply was connected to the point electrode via a series resistor $R = 6.85$ MΩ while the plate electrode was grounded (figure 1). The velocity of the air flow was about 0.5 m s^{-1}, parallel to the inter-electrode axis. The radius of curvature of the anode tip was of the order of 100 μm. The discharge voltage was measured by a HV probe (Tektronix P6015A) and the discharge current was measured by a current monitor (Pearson Electronics 2877 1 V A^{-1}) and by a 50 Ω resistor shunt. The voltage and current signals were recorded by a digitizing oscilloscope (Tektronix DPO 4104 bandwidth 1 GHz, or Tektronix TDS2024 with bandwidth 200 MHz).

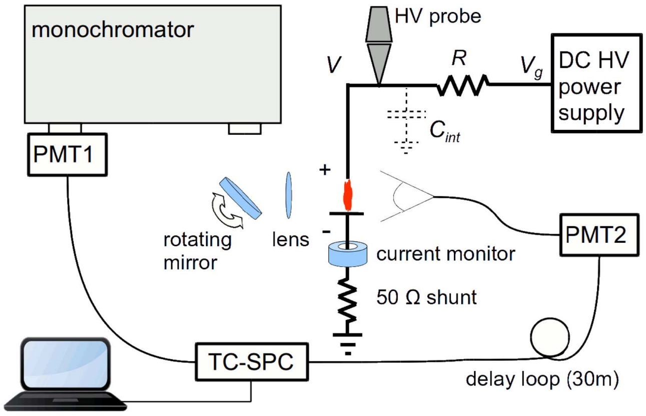

Figure 1. Schematic of the experimental setup, PMT—photo multiplier, TC-SPC—time correlated single photon counting board, R—external resistor, V—measured voltage, V_g—generator voltage.

The CCS was used to explore the entire evolution of the TS discharge. The emission from the discharge corresponding to the second positive system (SPS) of N_2 (0-0 transition at 337.1 nm), the first negative system (FNS) of N_2^+ (0-0 transition at 391.4 nm), and the emission lines of atomic oxygen (777.1 nm) and nitrogen (746 nm) were recorded. The CCS method was described elsewhere [34, 35], so only specific features of the set-up used in this study are described.

The idea of CCS is to accumulate single photons together with their time information from high-frequency repetitive discharge events. The time information of each photon is determined from its correlation to the integral light pulse of the same discharge, i.e. cross-correlation method. Therefore, the light pulses are investigated by two photomultipliers (PMTs). The PMT 1 detects the single photons after spatial and spectral separation, while PMT 2 defines the relative timescale of the light pulses being investigated. Both pulses are processed by the time-correlated single photon counter (TC-SPC, details being described elsewhere [32, 34]). To enable proper data acquisition in the reversed start-stop mode of the TC-SPC, the PMT 2 signal is delayed by a delay box (not shown) and an additional coaxial cable loop (30 m). The spectral resolution of the main-signal (PMT 1) is given by diffraction in a Czerny–Turner type monochromator with adjustable entrance and exit slits, grating with 1200 grooves mm^{-1} (blaze 300 nm). The spatially resolved acquisition of the temporally resolved discharge luminosity curves is achieved by an automatic scanning procedure. Therefore, the main-signal is imaged on the entrance slit of the monochromator via an achromatic lens and a rotating mirror. The rotating mirror and the TC-SPC card are both controlled by a scanning device (not shown in figure 1)

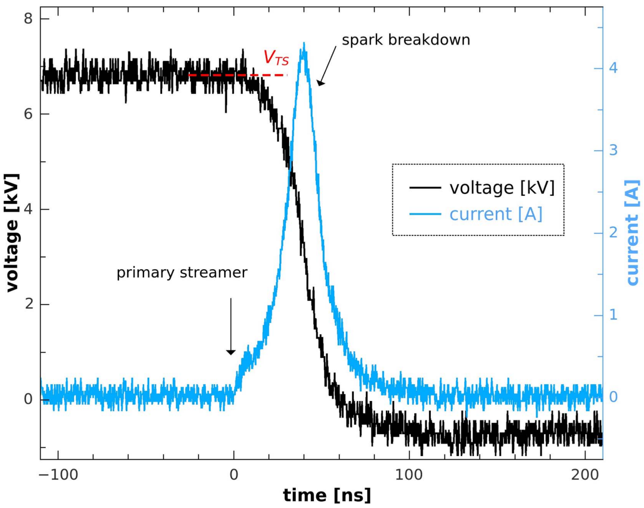

Figure 2. Typical waveforms of transient spark discharge (positive polarity, repetition frequency 8–10 kHz, gap 4 mm, Tektronix DPO 4104).

enabling the controlled spatially and temporally resolved data acquisition.

3. Results

3.1. Electrical discharge characteristics

When the HV applied to the point electrode V is progressively increased, a transition from streamer-corona to TS occurs when a characteristic voltage V_{TS} is achieved. The formation of the TS happens after a primary streamer crossed the whole gap and manifests itself in the generation of a conductive plasma channel. The plasma current discharges the internal capacitance C_{int} ($\sim$20 pF) of the electrical circuit. The corresponding current is given by

$$I(t) \approx -C_{\mathrm{int}} \frac{\mathrm{d}V}{\mathrm{d}t} \tag{1}$$

and reaches a maximum value in the range of a few Amps. Due to discharging of the internal capacity and the resistive fall on the external resistance, the applied voltage drops to zero leading to discharge decay (figure 2). This is followed by a relaxation phase, where the internal capacitance of the circuit is recharged by the growing potential V on the point electrode. A new TS pulse is initiated when V reaches the breakdown voltage V_{TS} again. Thus, the TS is based on the repetitive charging and discharging of C_{int} with a characteristic frequency f, which is given by the values of C_{int} and R as well as the generator voltage V_{g} [14]:

$$f = \frac{1}{RC_{\mathrm{int}} \ln\left\{\dfrac{V_{\mathrm{g}}}{V_{\mathrm{g}} - V_{\mathrm{TS}}}\right\}}. \tag{2}$$

However, it must be emphasized that the TS repetition frequency is not perfectly regular as each TS pulse appears at a slightly different value of V_{TS} [16]. Therefore, only averaged TS repetition frequency can be defined. For the set-up used in this study, the average TS repetition frequency is adjustable in the range 1–10 kHz. Further increase of frequency above 10 kHz was not possible, because the increase of f is accompanied by the increase of the mean current, and the TS tends to transit into a high pressure glow discharge at mean currents above 1.5 mA. The glow discharge regime is described in more detail in [36–40].

Since this study is intended to the investigation of 'memory' effects occurring in the TS discharge, experiments were focused on conditions where the average frequency was close to 10 kHz. In fact, the TS repetition frequency varied in the range 8–10 kHz, with the mean current between 1.3 and 1.4 mA. In order to keep the TS frequency as close to 10 kHz as possible, the generator voltage was tuned in the range 12.3–12.5 kV. The CCS study of breakdown mechanism in TS at lower frequencies was not possible due to long and variable streamer-to-spark transition time. Moreover, even the repetition frequency 8–10 kHz is relatively low to accumulate a sufficient amount of photons in a reasonable accumulation time.

3.2. CCS records

Figure 3 shows an averaged TS current pulse obtained at a repetition frequency in the range 8–10 kHz and correlates it with the measured luminosity distribution as obtained by CCS for the selected spectral band of the SPS and oxygen atomic line (777.1 nm), with a temporal resolution of about 60 ps and a spatial resolution (i.e. along the discharge inter-electrode axis) of 100 μm. A cathode directed (or primary) streamer starts in the region in the proximity of the anode and reaches the cathode at about 8 ns. This phase corresponds with an increasing but still relatively low current. Please note that the single shot (i.e. not averaged) current pulse in figure 2 shows a small local maximum of about 1 A in the range 0–20 ns. The transition to the spark starts at about 20 ns and is characterized by an axially uniform light emission and the formation of the higher current peak (time $\sim$20–60 ns in figure 2). The emission of the TS spark phase is dominated by the emission of atomic lines (O^* and N^*, the latter not shown as it is similar to O^*). The FNS signal was also detected. Obviously, this phase is characterized by a highly ionized plasma channel, with excited species generated probably by stepwise processes.

During the primary streamer (time $\sim$0–8 ns in figure 4), the emission of the SPS dominates, but a weak emission of the FNS and very weak emission of excited atomic oxygen are also observed. The interesting fact of the FNS being constantly ahead of the SPS signal during the streamer propagation was discussed and clarified in detail in [41]. The transition to the spark (developed at time $\sim$13–27 ns in figure 4) is observed within about 5 ns after the primary streamer bridges the electrodes. The spark itself is preceded not only by the primary streamer, but also by a feature (times $\sim$8–11 ns in figure 4) that probably represents a secondary streamer [42]. Some CCS records also indicate the presence of a return stroke between the primary and the secondary streamer, such as obtained by Gerling *et al* in argon TS [43].

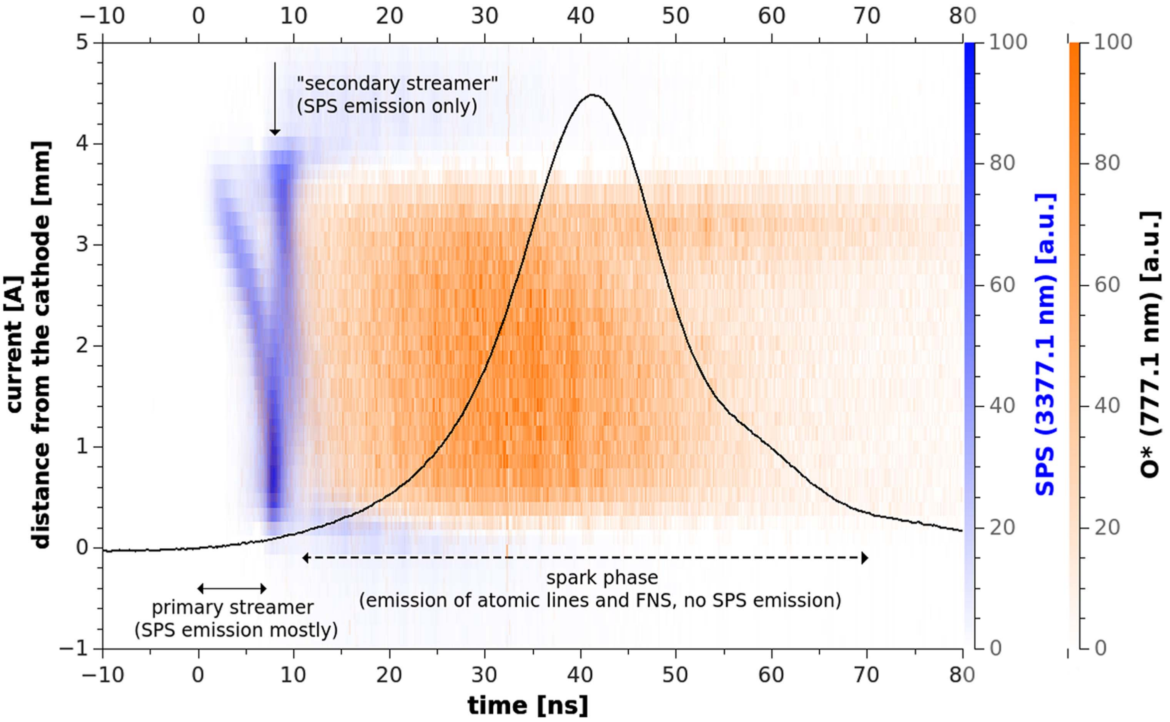

Figure 3. Cross-correlation spectroscopy record of the TS evolution overlapped with the averaged TS current pulse (recorded on Tektronix DPO 4104), positive polarity, anode at the top, repetition frequency 8–10 kHz, gap 4 mm.

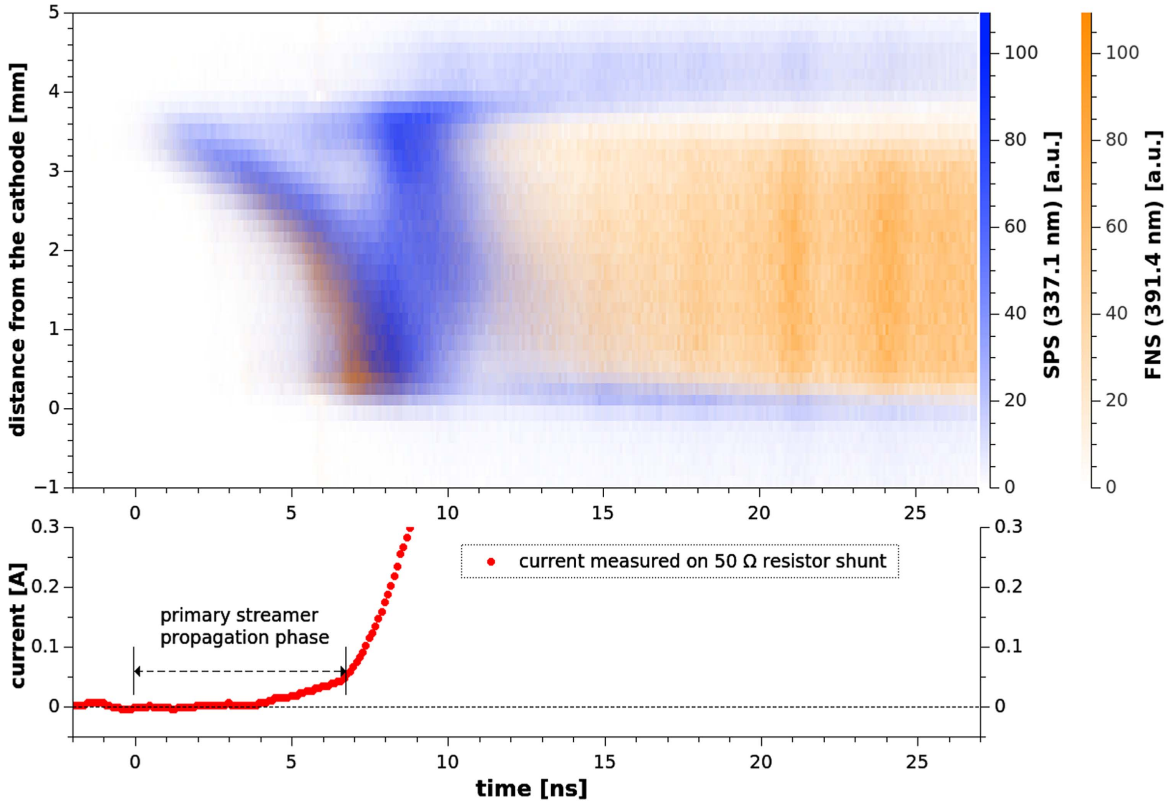

Figure 4. Cross-correlation spectroscopy record of the TS evolution for the selected spectral band of the N_2 SPS and N_2^+ FNS with the single pulse TS current waveform (recorded on 50 Ω resistor shunt, Tektronix TDS2024), positive polarity, anode at the top, repetition frequency 8–10 kHz, gap 4 mm.

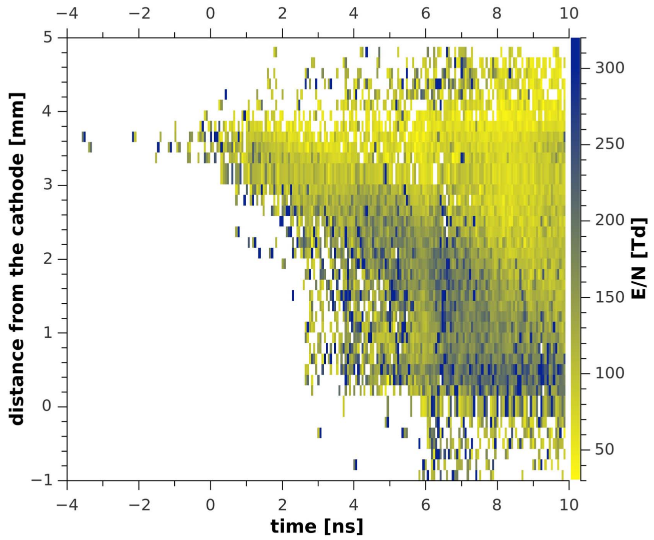

Figure 5. Spatiotemporal distribution of the reduced electric field strength E/N during the primary streamer phase of the TS discharge in atmospheric pressure air (positive polarity, anode at the top, repetition frequency 8–10 kHz, gap 4 mm). E/N calculated from the emissions of N_2 SPS and N_2^+ FNS.

However, it remains uncertain due to shorter time scales of discharge evolution in air and limited sensitivity of the CCS given by Poisson statistics (we cannot see weaker events because of stronger signal from the primary and secondary streamer).

3.3. Calculation or reduced electric field strength

Using the FNS and SPS signals, the reduced electric field strength (E/N) during the primary streamer phase of the TS discharge was determined (figure 5). The method of reduced electric field strength determination in weakly ionized phases of discharge development from the intensity ratio of the spectral bands of molecular nitrogen (FNS and SPS systems) is well known [32–35]. Recently, the details, advantages and limitations of this method have been discussed in [44, 45]. The issue of fast electron velocity distribution function relaxation for different electric field magnitudes, and the influence of the gas temperature were discussed for atmospheric pressure air [44]. The influence of the different quenching parameters and calibration dependences of the FNS to SPS signal intensity ($R_{\mathrm{FNS/SPS}}$) as function of E/N were described in [45].

Here, the relative reduced electric field strength was determined using the differential form of the intensity ratio dependence on reduced electric field strength $R_{\mathrm{FNS/SPS}}$ (E/N) as given in [45]. The following equation was used:

$$\left(\frac{I_{\mathrm{FNS}}/\tau_{\mathrm{eff}}^{\mathrm{FNS}} + \mathrm{d}I_{\mathrm{FNS}}/\mathrm{d}t}{I_{\mathrm{SPS}}/\tau_{\mathrm{eff}}^{\mathrm{SPS}} + \mathrm{d}I_{\mathrm{SPS}}/\mathrm{d}t}\right)\frac{\tau_{\mathrm{eff}}^{\mathrm{FNS}}}{\tau_{\mathrm{eff}}^{\mathrm{SPS}}} = R_{\mathrm{FNS/SPS}}(E/N), \qquad (3)$$

where I_{FNS} and I_{SPS} denote the measured intensities of FNS and SPS, respectively. Next, ${\tau_{\mathrm{eff}}}^{\mathrm{FNS}} = 0.045$ ns and ${\tau_{\mathrm{eff}}}^{\mathrm{SPS}} = 0.640$ ns are effective lifetimes of excited $N_2^+(B)$ and $N_2(C)$ states, respectively, in the atmospheric pressure air [44].

The absolute values of the reduced electric field were obtained by comparing the applied voltage and computed integral of the determined electric field over the gap. Similarly to the ultra-fast breakdown in Trichel pulse negative corona and single filament barrier discharges in atmospheric pressure air, the condition of local field approximation is also fulfilled [44].

The spatio-temporally resolved development of E/N in the cathode directed streamer is shown in figure 5. The reduced electric field starts to rise already in the close vicinity of the pin anode. Approximately at 1 mm distance from the anode the streamer has created a space charge field exceeding 150 Td. This value increases up to the approximately 300 Td at the streamer impact onto the cathode. On the way of the streamer head to the cathode the reduced electric field is around 250 Td.

This method is not applicable for the next phases of the TS discharge, because only the SPS emission and no FNS emission are observed during the secondary streamer. During the spark phase on the contrary, only the FNS emission and atomic lines were detected, but no SPS emission. Moreover, this method is only suitable if direct electron impact processes dominate in the studied plasma. In the TS during the spark phase, the stepwise processes generating excited N_2^+ ions are much more likely since the electron density is high [18].

4. Discussion

The average primary streamer propagation velocity is $\sim 6 \times 10^7$ cm s^{-1}, which is in agreement with previously observed values [46–48], despite the fact that figure 4 shows considerably more dispersion in the paths of the streamers than previous CCS studies [32, 44]. This can be explained by the spatial jitter of the TS discharge. Individual streamers do not necessarily follow the same path and thus, their propagation times certainly differ.

The calculated reduced electric field strength during the primary streamer phase of the TS ($\sim$300 Td in maximum at the contact with cathode, with the error of the method of about 20%) is lower than usually obtained by modeling studies of positive streamer in air [8, 49, 50]. This can be explained by high degree of pre-ionization caused by the spark phase of the TS in connection with the relatively high repetition frequency of the discharge. The high electron density in the spark phase leads to significantly higher residual electron density in the gap. This results in lower maximum reduced electric field strength in the streamer head. This is consistent with the simulation results of Bourdon *et al* [12], showing influence of the pre-ionization degree on the positive streamer characteristics, with maximum field in streamer's head around 200 Td only. It could be also related to relatively blunt anode, as shown by Kulikovsky [11]. Even though, the reduced electric field strength above 200 Td is enough for efficient direct electron impact ionization, and it can explain why electron density as high as 10^{14} cm^{-3} can be achieved in the discharge channel right after the primary streamer bridges the electrodes [18].

The E/N in the discharge channel created by the primary streamer is certainly much lower. Previously, the average axial E/N in TS during the streamer-to-spark transition phase was estimated to be around 60–70 Td, assuming homogeneous axial E/N distribution [16]. In reality, the assumption of homogeneous axial E/N is not correct and the field is certainly higher near the anode, where it leads to the formation of the secondary streamer (see figure 4, time around 10 ns).

The name 'secondary streamer' was given by Loeb who suggested it was a new ionization wave [6], but it is a result of non-homogeneous distribution of the plasma conductivity along the gap. Lower plasma conductivity results in E/N increase near the anode [42, 51–53], where it can reach value above 80 Td [52]. This is still not high enough for direct electron impact ionizations and consequently no FNS emission is observed during this phase. However, it is high enough for the generation of excited molecular nitrogen observed as 'the secondary streamer'.

The non-homogeneous axial distribution of E/N in the channel created by the primary streamer can be explained by the SPS emission intensity, which increases as the primary streamer propagates from the anode towards the cathode. The $N_2(C)$ excited states are mostly generated by the direct electron impact excitation of the ground state molecular nitrogen during this phase [41]. Thus, the increase of the SPS emission intensity closer to the cathode during the primary streamer phase indicates a non-homogeneous distribution of electron density along the filament created by the primary streamer, with increasing electron density towards the cathode. The conductivity of weakly ionized plasma is proportional to the electron density and should be thus higher near the cathode. As a result, the axial distribution of the electric field must be non-homogeneous after the primary streamer bridges the electrodes, with enhancement near the anode, where the plasma conductivity is lower.

To extend the region with the elevated field towards the cathode, the decrease of gas density near cathode is needed, as shown in the model of Bastien and Marode [51]. In the situation investigated here, the propagation of the secondary streamer was so fast (figure 4) that the decrease of gas density can probably be neglected. As a result, the extension of the 'high field' region from the anode towards the cathode is not possible. It would lead to the smoothening of the axial E/N distribution, i.e. in our case, the increase of E/N near the cathode is accompanied by the decrease of E/N near the anode. With the final homogeneously distributed E/N below 80 Td, no additional $N_2(C)$ states are generated and the secondary streamer (light emitting region) disappears without its propagation through the whole gap. This can probably explain why the secondary streamer stopped approximately 1 mm before the cathode (time ~10 ns in figure 4). Afterwards, the field probably remains weak during the whole spark phase, as can be also deduced from the fast decrease of the discharge voltage (figure 2), with no significant generation of $N_2(C)$ excited states, and consequently no SPS emission.

If the electric field is too low for the generation of $N_2(C)$, it is also too low for efficient generation of electrons by direct electron-impact reactions with N_2 and O_2 molecules. The plasma should enter the decay phase, with electron density quickly decreasing due to electron attachment and electron–ion recombination processes. This has been concluded from TS studies at lower frequencies, where the current after the primary streamer starts to drop [16]. However, no current drop after the primary streamer in the TS is obtained at 10 kHz (figure 2).

Both at low and higher TS repetition frequencies, the plasma bridge generated by the primary streamer enabled the passage of ohmic current through the discharge that does not need high E/N. The current delivered by the power supply is limited by external resistor to ~1 mA, but the measured current right after the streamer is above 100 mA. In the first approximation, we thus need to consider only the current due to partial discharging of the internal capacity of the used electric circuit. The rate of discharging depends on the plasma channel conductivity that is proportional to the electron density. In order to explain further evolution of the discharge current, i.e. whether the discharging of C_{int} will slow down or it will smoothly increase to form the spark current pulse, we need to answer the question of electron density evolution inside the generated plasma channel. We thus assume that further discharge current evolution is driven by the processes in the plasma volume.

Different evolution of current and electron density during the streamer-to-spark phase means that the ratio between electron production and loss processes changes with increasing TS repetition frequency. At ~10 kHz, the net electron production rate is always positive, despite low reduced electric field strength. This can be achieved either by an enhancement of electron production mechanisms, or by deceleration of electron loss processes. Unfortunately, we are not able to distinguish which scenario is more accurate, but we assume that memory effects induced by previous TS pulses: gas heating up to 500–600 K [16], and changes in the gas composition, can explain both possibilities.

The electron attachment rate decreases if the gas density is reduced by heating. In addition, the accumulation of O species, as also obtained in nanosecond repetitive pulsed discharge at 10 kHz [54], would accelerate the electron detachment reactions [55]. Moreover, O_4^+ ions are decomposed at elevated temperature [10, 56], which suppresses their recombination with electrons. This recombination process is an important electron sink channel at 300 K [10, 55], because its rate coefficient is about two orders of magnitude higher than the rate coefficients of reactions with O_2^+ and N_2^+ ions [57, 58]. Altogether, these processes inhibit the electron losses.

Concerning the electron production processes, one possible explanation is the generation of charged particles by the ionization of species with lower ionization threshold energy, such as $N_2(A)$ or O. These species can be considered as the most typical 'successors' of the $N_2(C)$ excited states generated by the primary (mostly near the cathode) and the secondary (mostly near the anode) streamers:

$$N_2(C) \rightarrow N_2(B) \rightarrow N_2(A), \tag{4}$$

$$N_2(C, B, A) + O_2 \rightarrow N_2(X) + O + O. \quad (5)$$

Moreover, as we already mentioned, we assume that the density of accumulated atomic oxygen from previous pulses grows with increasing TS repetition frequency.

Thanks to the high electron density ($>10^{14}$ cm^{-3}), the stepwise ionization processes probably also plays a significant role in the generation of electrons. At lower frequencies, the electron attachment dominates and the importance of the stepwise ionization processes diminishes quickly due to decreasing electron density. At 10 kHz, assuming low attachment rate, the stepwise ionization processes can create a positive feedback, because their importance should increase with increasing electron density. Thus, the increase in the electron density should result to the faster generation of electrons by the stepwise pathways. Increasing electron density means higher plasma channel conductivity and faster discharging of C_{int}, resulting to the spark current pulse formation.

5. Conclusions

We investigated the streamer-to-spark transition mechanism in the TS discharge in atmospheric pressure air using CCS. The TS is a self-pulsing discharge initiated by a primary streamer followed by a short spark current pulse. The TS mean repetition frequency can be controlled in the range 1–10 kHz by the applied voltage, but the self-pulsing frequency is not regular.

The results show that at TS repetition frequency ~10 kHz, the transition from the primary streamer to the spark proceeds within about 10 ns. Such fast transition could be attributed to several memory effects, causing a low net electron attachment rate and faster propagation of the secondary streamer. First, the gas pre-heating decreases the density of the gas and thus, decreases the rate of electron attachment. Next, the accumulation of species such as oxygen atoms generated by the previous TS pulses can enhance electron detachment reactions.

With low net electron attachment rate, even relatively slow stepwise ionization processes could be sufficient to cause the transition to the spark and the breakdown after the secondary streamer. Another possible explanation is the generation of charged particles by ionization of species with lower ionization threshold energy, such as $N_2(A)$ or O. Further research is required, including kinetic modeling to verify this hypothesis. The rapid production of the light emission generated by atomic oxygen in the ionized channel after the secondary streamer is also worth of further deeper analysis. In future, we also hope to explain weak SPS emission that seems to be out of the gap, while there is no SPS emission inside the gap during the spark phase of TS.

The CCS was demonstrated to be a suitable technique for the investigation of such self-pulsing and erratically appearing discharges enabling to reveal elementary mechanisms of electron production and losses and consequently streamer to spark transition in non-homogeneous electric field in atmospheric pressure air. This study can potentially serve as a reference for more detailed future spectroscopic investigations of streamer to spark transition in air.

Acknowledgments

The research leading to these results has received funding from the European Union Seventh Framework Programme (FP7/2007-2013) under grant agreement n°316216. Effort was also sponsored by the Slovak Research and Development Agency APVV-0134-12, Slovak grant agency VEGA 1/0918/15, and Czech Science Foundation project Nr. 15-04023S. This research has also been supported by the project CZ.1.05/2.1.00/03.0086 funded by European Regional Development Fund and project LO1411 (NPU I) funded by Ministry of Education Youth and Sports of Czech Republic.

References

[1] Peek F W Jr 1929 *Phenomena in High Voltage Engineering* (New York: McGraw-Hill)
[2] Llewellyn-Jones F 1966 *Ionization and Breakdown in Gases* (London: Methuen)
[3] Meek M J and Craggs J D 1978 *Electrical Breakdown of Gases* (New York: Wiley)
[4] Meek J M 1940 *Phys. Rev.* **57** 722
[5] Raether H 1964 *Electron Avalanches and Breakdown in Gases* (London: Butterworths)
[6] Loeb L B 1965 *Electrical Coronas* (Berkeley, CA: University of California Press)
[7] Marode E 1975 *J. Appl. Phys.* **46** 2005
[8] Morrow R and Lowke J J 1997 *J. Phys. D: Appl. Phys.* **30** 614–27
[9] Larsson A 1998 *J. Phys. D: Appl. Phys.* **31** 1100
[10] Aleksandrov N L and Bazelyan E M 1999 *Plasma Sources Sci. Technol.* **8** 285
[11] Kulikovsky A A 2001 *IEEE Trans. Plasma Sci.* **29** 313
[12] Bourdon A, Bonaventura Z and Celestine S 2010 *Plasma Sources Sci. Technol.* **19** 034012
[13] Machala Z, Janda M, Hensel K, Jedlovský I, Leštinská L, Foltin V, Martišovitš V and Morvová M 2007 *J. Mol. Spectrosc.* **243** 194
[14] Janda M, Martišovitš V and Machala Z 2011 *Plasma Sources Sci. Technol.* **20** 035015
[15] Gerling T, Hoder T, Bussiahn R, Brandenburg R and Weltmann K-D 2013 *Plasma Sources Sci. Technol.* **22** 065012
[16] Janda M, Machala Z, Niklová A and Martišovitš V 2012 *Plasma Sources Sci. Technol.* **21** 045006
[17] Gerling T, Hoder T, Brandenburg R, Bussiahn R and Weltmann K-D 2013 *J. Phys. D: Appl. Phys.* **46** 145205
[18] Janda M, Martišovitš V, Dvonč L, Hensel K and Machala Z 2014 *Plasma Sources Sci. Technol.* **23** 065016
[19] Naidis G V 2009 *Eur. Phys. J. Appl. Phys.* **47** 22803
[20] Pai D Z, Lacoste D A and Laux C O 2010 *Plasma Sources Sci. Technol.* **19** 065015
[21] Pai D Z, Lacoste D A and Laux C O 2010 *J. Appl. Phys.* **107** 093303
[22] Bazelyan E M and Raizer Y P 2000 *Lightning Physics and Lightning Protection* (Bristol: IOP Publishing Ltd)
[23] Jeremy A, Riousset A, Pasko V P and Bourdon A 2010 *J. Geophys. Res.* **115** A12321

[24] Gordillo-Vazquez F J and Luque A 2010 *Geophys. Res. Lett.* **37** 16809

[25] Luque A, Stenbaek-Nielsen H C, McHarg M G and Haaland R K 2016 *J. Geophys. Res. (Space Phys.)* **121** 2431–49

[26] Hoeft H, Kettlitz M, Becker M M, Hoder T, Loffhagen D, Brandenburg R and Weltmann K-D 2014 *J. Phys. D: Appl. Phys.* **47** 465206

[27] Le Delliou P, Tardiveau P, Jeanney P, Bauville G and Pasquiers S 2011 *IEEE Trans. Plasma Sci.* **39** 2686

[28] Bentaleb S, Tardiveau P, Moreau N, Jeanney P, Jorand F and Pasquiers S 2011 *IEEE Trans. Plasma Sci.* **39** 2236

[29] Jánský J, Le Delliou P, Tholin F, Bonaventura Z, Tardiveau P, Bourdon A and Pasquiers S 2011 *IEEE Trans. Plasma Sci.* **39** 2106

[30] Brandenburg R, Hoder T and Wagner H-E 2008 *IEEE Trans. Plasma Sci.* **36** 1318

[31] Brandenburg R *et al* 2013 *J. Phys. D: Appl. Phys.* **46** 464015

[32] Kozlov K V, Wagner H-E, Brandenburg R and Michel P 2001 *J. Phys. D: Appl. Phys.* **34** 3164–76

[33] Wagner H-E, Brandenburg R, Kozlov K V, Sonnenfeld A, Michel P and Behnke J F 2003 *Vacuum* **71** 417

[34] Becker W 2005 *Advanced Time-Correlated Single Photon Counting Techniques* (Berlin: Springer)

[35] Wagner H-E, Kozlov K V and Brandenburg R 2008 *Low Temperature Plasmas* ed R Hippler *et al* vol 1 (Weinheim: Wiley-VCH) p 271

[36] Akishev Y S, Deryugin A A, Kochetov I V, Napartovich A P and Trushkin N I 1993 *J. Phys. D: Appl. Phys.* **26** 1630

[37] Machala Z, Morvová M M, Marode E and Morva I 2000 *J. Phys. D: Appl. Phys.* **33** 3198

[38] Yu L, Laux C O, Packan D M and Kruger C H 2002 *J. Appl. Phys.* **91** 2678

[39] Staack D, Farouk B, Gutsol A and Fridman A 2005 *Plasma Sources Sci. Technol.* **14** 700

[40] Akishev Y, Grushin M, Karalnik V, Petryakov A and Trushkin N 2010 *J. Phys. D: Appl. Phys.* **43** 075202

[41] Hoder T, Bonaventura Z, Bourdon A and Simek M 2015 *J. Appl. Phys.* **117** 073302

[42] Sigmond R S 1984 *J. Appl. Phys.* **56** 1355

[43] Gerling T, Nastuta A V, Bussiahn R, Kindel E and Weltmann K-D 2012 *Plasma Sources Sci. Technol.* **21** 034012

[44] Hoder T, Loffhagen D, Vorac J, Becker M M and Brandenburg R 2016 *Plasma Sources Sci. Technol.* **25** 025017

[45] Hoder T, Šimek M, Bonaventura Z, Prukner V and Gordillo-Vázquez F J 2016 *Plasma Sources Sci. Technol.* **25** 045021

[46] Naidis G V 1996 *J. Phys. D: Appl. Phys.* **29** 779–83

[47] Allen N L and Mikropoulos P N 1999 *J. Phys. D: Appl. Phys.* **32** 913–9

[48] Tardiveau P, Marode E and Agneray A 2002 *J. Phys. D: Appl. Phys.* **35** 2823–9

[49] Kulikovsky A A 1997 *J. Phys. D: Appl. Phys.* **30** 441–50

[50] Kulikovsky A A 1998 *IEEE Trans. Plasma Sci.* **26** 1339–46

[51] Bastien F and Marode E 1985 *J. Phys. D: Appl. Phys.* **18** 377

[52] Marode E, Djermoune D, Dessante P, Deniset C, Segur P, Bastien F, Bourdon A and Laux C 2009 *Plasma Phys. Control. Fusion* **51** 124002

[53] Ono R and Oda T 2007 *J. Phys. D: Appl. Phys.* **40** 176

[54] Stancu G D, Kaddouri F, Lacoste D A and Laux C O 2010 *J. Phys. D: Appl. Phys.* **43** 124002

[55] Dvonč L and Janda M 2015 *IEEE Trans. Plasma Phys.* **43** 2562–70

[56] Kossyi I A, Kostinsky A Y, Matveyev A A and Silakov V P 1992 *Plasma Sources Sci. Technol.* **1** 207

[57] Mitchell J B A 1990 *Phys. Rep.* **186** 215

[58] Johnsen R 1993 *J. Chem. Phys.* **98** 5390